Pediatric multifocal liver lesions evaluated by MRI

Majed Almotairi, Kamaldine Oudjhane, Govind B Chavhan

Department of Diagnostic Imaging, The Hospital for Sick Children, University of Toronto, Toronto, Ontario, Canada

Correspondence: Dr. Govind B Chavhan, Department of Diagnostic Imaging, The Hospital for Sick Children, University of Toronto, 555 University Avenue, Toronto, Ontario - M5G 1X 8, Canada. E-mail: govind.chavhan@sickkids.ca

Abstract

Objective: The purpose of this study is to present our experience with MRI evaluation of multifocal liver lesions in children and describe the MRI characteristics of these lesions. **Patients and Methods:** A retrospective review of consecutive MRI exams performed for the evaluation of multiple liver lesions between 1 January 2007 and 31 December 2012 was done to note the number of lesions, the size of the largest lesion, MR signal characteristics, and background liver. Final diagnosis was assigned to each case based on pathology in the available cases and a combination of clinical features, imaging features, and follow-up in the remaining cases. **Results:** A total of 48 children (22 boys, 26 girls; age between 3 months and 18 years with average age 10.58 years and median age 11 years) were included in the study. Totally 51 lesion diagnoses were seen in 48 children that included 17 focal nodular hyperplasia (FNH), 8 hemangiomas, 7 metastases, 6 regenerative nodules, 3 adenomas, 3 abscesses, and one each of angiomyolipoma, epithelioid hemangioendothelioma, focal fatty infiltration, hepatocellular carcinoma, hepatic infarction, nodular regenerative hyperplasia, and hepatic cyst. Background liver was normal in 33, cirrhotic in 10, fatty in 3, and siderotic in 2 children. Most FNH, hemangiomas, and regenerative nodules showed characteristic MRI features, while metastases were variable in signal pattern. **Conclusion:** Many commonly seen multifocal liver lesions in children have characteristic MRI features. MRI can help to arrive at reasonable differential diagnoses for multifocal liver lesions in children and guide further investigation and management.

Key words: Children; MRI; multifocal liver lesions

Introduction

Multifocal liver lesions in children are infrequently seen in routine practice. Imaging plays an important role in the management. Most of these lesions are initially detected on ultrasound (USG). The USG features are generally nonspecific. Nowadays, these lesions in children are being routinely evaluated by MRI. In our experience, MRI helps to characterize these lesions and narrow the differential diagnosis. In some cases, in combination with clinical features, MRI helps to avoid biopsy for the diagnosis. There are a few reviews on imaging of multifocal liver lesions and liver lesions in general in children.[1-4] However, to the best of our knowledge, there are no original studies published on imaging of multifocal liver lesions in children presenting the actual experience in daily practice. In this manuscript, multiple liver lesions of the same pathologic entity as well as multiple lesions of different pathologic entity are included and all are referred as multifocal liver lesions.

The purpose of this study is to present our experience with MRI evaluation of multifocal liver lesions in children at our institution. This study also aims at describing the MR imaging features of common and uncommon multifocal liver lesions.

Access this article online	
Quick Response Code:	Website: www.ijri.org
	DOI: 10.4103/0971-3026.161466

Patients and Methods

Institutional Research Ethics Board approval and waiver for consent were obtained for this study. We retrospectively reviewed consecutive liver MRI in children (<18 years) with multifocal liver lesions performed between January 2007 and December 2012. A radiology fellow compiled

the list of liver and abdominal MRI from picture archiving and communication system (PACS) using the filters "MRI Abdomen" and "MRI Liver" in the examination column. He then prepared the final list of MR examinations by looking at the reports mentioning more than two liver lesions. Non-diagnostic studies and those with a single liver lesion were excluded.

MRI technique

MR imaging was performed using either a 1.5 T Siemens (Avanto; Siemens Medical system, Erlangen, Germany) or 1.5 T and 3 T Philips (Achieva; Philips Medical system, Best, the Netherlands) MRI scanners. Children below 6 years of age were scanned under general anesthesia. Acquired sequences included a combination of coronal single-shot T2W, axial T1W gradient-echo sequence with in- and out-phase, axial T2W fast spin-echo with respiratory triggering, balanced SSFP (steady state free precession) (True FISP/bTFE), diffusion-weighted images, pre-contrast axial and coronal T1W 3D gradient-echo sequence [volume interpolated body examination (VIBE) (Siemens)/T1W high-resolution isotropic volume examination (THRIVE) (Philips)]. Post-contrast images were obtained including axial T1W 3D gradient-echo sequence in arterial, portal venous, and equilibrium phases during dynamic injection of gadolinium-based contrast media and axial T1 fast spin-echo with fat saturation at 5 min after contrast injection. The typical scan time for T1W 3D gradient-echo sequence ranged between 15 and 20 s. The dynamic imaging was performed using manual timing with arterial phase starting at 16 s, portal venous phase at 55 s, and equilibrium phase at 2 min.

Imaging analysis

All MRIs were evaluated by two pediatric radiologists (GBC with 7 and KO with 27 years of experience in reading pediatric body MRI, respectively) independently. Any disagreements were resolved by consensus. Both radiologists were blinded to clinical details and final diagnosis. The number (number of the lesions was noted up to 10; more than 10 lesions were rounded to 10), size, and signal characteristics of lesions were noted on T1W, T2W, in- and out-phase, arterial phase, portal venous phase, and equilibrium phase images. They also recorded their most likely diagnosis and a differential. The final "imaging diagnosis" was assigned to each case by consensus reading.

Chart review and final diagnosis

Patient charts were reviewed by a radiology fellow after the completion of the imaging review for specific clinical details including known primary tumor, follow-up, and histology if biopsy was available. The final lesion diagnosis was based on histology if available. In cases without biopsy, the diagnosis was based on characteristic imaging features, mainly on MRI, clinical features, and any available corroborative evidence such as lesion stability on follow-up imaging. The period between the first imaging on which the lesion was detected and the latest available imaging was considered follow-up period for lesion size change. Imaging modalities used for lesion stability included MRI, USG, and CT scan. Stability in size over a period and/or gradual marginal growth supports benign nature of the lesion.

Results

A total of 48 children (22 boys, 26 girls; age between 3 months and 18 years with average age 10.58 years) had MRI exams for the evaluation of multiple liver lesions during the study period.

Associated or background conditions in 48 children are summarized in Table 1. Only 7/48 children were otherwise healthy at presentation without significant associated or previous disease conditions.

Overall, 19/48 children had >10 lesions, 12/48 had 5-9 lesions, and 17/48 had <4 lesions. The largest lesion ranged between 0.4 × 0.5 cm and 14.3 × 8.9 cm. The appearance of the background liver parenchyma on MRI was normal in

Table 1: Background/associated diseases in children (*N*=48)

Category	Number	Number-individual entities
Previous or current malignancy	19	6- Neuroblastoma 1 each- atypical teratoid rhabdoid tumor of the brain, adrenocortical carcinoma, chronic myeloid leukemia, desmoplastic small round cell tumor of the abdomen, desmoplastic small round cell tumor of the mesentery, hepatoblastoma, lymphoma, medulloblastoma, papillary renal cell carcinoma, ovarian rhabdomyosarcoma, sarcomas*, Wilms' tumor, and undifferentiated sarcoma of the kidney
Underlying liver disease	13	2 each- biliary atresia and glycogen storage disorder 1 each- agenesis of portal vein, Alagille syndrome, Budd-Chiari syndrome with polyarteritis nodosa, chronic hepatitis B, congenital hepatic fibrosis, cystic fibrosis with portal hypertension, hypoplastic left heart syndrome with Fontan procedure, tyrosinemia, and primary sclerosing cholangitis with ulcerative colitis
Systemic disorders or syndromes	7	2- Li-Fraumeni syndrome 1 each- epithelioid hemangioendothelioma, hyper IgE syndrome, Langerhans cell histiocytosis, neurofibromatosis type 1, and tuberous sclerosis
Others	2	1 each- meningitis and sensory neural hearing loss
Otherwise previously healthy	7	

*This child had two sarcomas, initially rhabdomyosarcoma of the popliteal fossa and later developed osteosarcoma of the femur

33/48 children, cirrhotic in 10/48, with fatty infiltration in 3/48, and siderotic in 2/48 children.

Standard of reference

The final diagnosis was based on pathology in 17/48 children. In 24/48 children, it was based on a combination of imaging, clinical features, and follow-up (follow-up period from 6 months to 5 years; average 26 months). The lesion stability or only marginal growth over the follow-up period was considered as one of the corroborative evidences for the benign nature of the lesion. In the remaining 7/48 children, the final diagnosis was based on imaging and clinical features.

Three of 48 children had two different types of hepatic lesions [adenoma and focal nodular hyperplasia (FNH); regenerative nodule (RN) and FNH; and FNH and hemangioma], giving 51 lesion diagnoses in 48 children. These are summarized in Table 2.

Focal nodular hyperplasia

Seventeen of 48 children (7 boys, 10 girls; age 2-17 years with average age 10.41 years) had multiple FNH. Three of the 17 children had biopsy-proven FNH. Ten of 17 children had previous history of cancer. The appearance of background liver parenchyma on MRI was normal in 12/17 children, with fatty infiltration in 1/17, and cirrhotic in 4/17. FNH in two of the children with cirrhotic appearance on MRI had biopsy correlation. Four of 17 children had >10 lesions, 6/17 had 5-9 lesions, and remaining 7/17 had <4 lesions. Most lesions were well-defined with the largest measuring 6.4 × 4 cm in transverse dimensions. Most FNH were iso-to-hypointense on T1W, slightly hyperintense on T2W, showed prompt arterial enhancement, and became iso-to-slightly hyperintense on portal venous phase and equilibrium phase images [Figure 1]. A few FNH in 6/17 children showed central scar. One child with Li–Fraumeni syndrome and previous history of astrocytoma had multiple biopsy-proven FNH that contained fat.

Hemangiomas

Eight of 48 children (2 boys, 6 girls; age from 3 months to 17 years with average age 8.66 years) had multiple hemangiomas. None of these cases had pathological confirmation. Three of these children were otherwise healthy and remaining one each had history of lymphoma, ovarian rhabdomyosarcoma, neurofibromatosis type 1, sensory neural hearing loss, and meningitis. Background liver had normal appearance on MRI in all children. Four of eight children showed >10 lesions, 3/8 had two lesions each, and one child had seven lesions. The largest lesion measured 1.3 × 2.2 cm. All lesions were hypo- or iso-intense on T1W, hyperintense on T2W, and showed prompt arterial enhancement and remained hyperintense to parenchyma on equilibrium phase images [Figure 2].

Table 2: Final diagnoses of multifocal liver lesions in 48 children (*N*=51)*

Number	Diagnosis
17	Focal nodular hyperplasia
8	Hemangioma
7	Metastases
6	Regenerative nodules
3	Adenoma
3	Abscess
1 each	Angiomyolipoma, epithelioid hemangioendothelioma, focal fatty infiltration, hepatocellular carcinoma, infarcts, nodular regenerative hyperplasia, and hepatic cysts

*Three children had two different types of lesions

Metastases

Seven of 48 children (5 boys, 2 girls; age from 7 months to 14 years with average age 8 years) had biopsy-proven metastases. Primary tumors included neuroblastoma (three instances) and papillary renal cell carcinoma, undifferentiated sarcoma of the kidney, adrenocortical carcinoma, and desmoplastic small round cell tumor of the abdomen (one case each). Background liver parenchyma had normal appearance in six children and was siderotic in one child. Four of seven children showed >10 lesions and remaining three showed <4 lesions with the largest measuring 14.3 × 8.9 cm. All lesions were hypointense on T1W and hyperintense on T2W images. Dynamic imaging was not available in three children. Enhancement pattern was variable in all phases with some showing hyper-enhancement and the others remaining hypointense to parenchyma on equilibrium. A few metastases in two children showed central scar, but none showed fat content [Figure 3].

Regenerative nodules

RNs were seen in 6/48 children (3 boys, 3 girls; age from 14 months to 17 years with average age 12.11 years), one of which had pathological confirmation from explanted liver. Associated conditions in these children included chronic myeloid leukemia, congenital hepatic fibrosis, hypoplastic left heart syndrome with Fontan procedure,

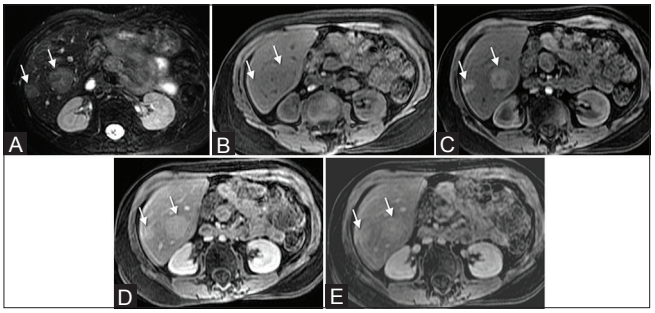

Figure 1 (A-E): Focal nodular hyperplasia (arrows) in a girl with previous history of rhabdomysarcoma. The lesions are slightly hyperintense on T2W fat suppressed (A) isointense on pre-contrast T1W 3D gradient-echo image (B) show avid enhancement on arterial phase (C) remain slightly hyperintense to parenchyma on portal venous phase (D) and become isointense to parenchyma on equilibrium phase image (E)

Langerhans cell histiocytosis, biliary atresia, and previously resected hepatoblastoma with cirrhosis in the residual liver. The hepatic parenchyma showed features of cirrhosis in four children, iron deposition in one child, and normal appearance in another one child. Three children showed >10 lesions, and remaining three children had five, -four, and three lesions, respectively. The largest nodule measured 2.6 × 3.5 cm, but most nodules were less than 2 cm in diameter [Figure 4]. All nodules were either iso- or hyperintense on T1W images. On T2W images, four children had hyperintense and two children had hypointense nodules. Enhancement pattern was variable with nodules showing hyper-enhancement on arterial phase in two children. Otherwise, the enhancement was predominantly isointense to the parenchyma on all phases.

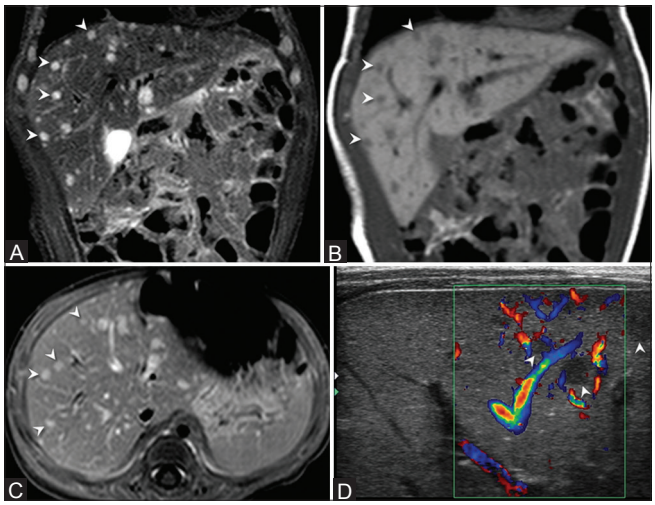

Figure 2 (A-D): Hemangiomas (arrowheads). Multiple small lesions are hyperintense on coronal STIR image (A) hypointense on coronal T1W image (B) and show homogeneous enhancement on post-contrast T1W fat sat image (C) The lesions are hypoechoic on ultrasound color image (D) and show peripheral vascularity

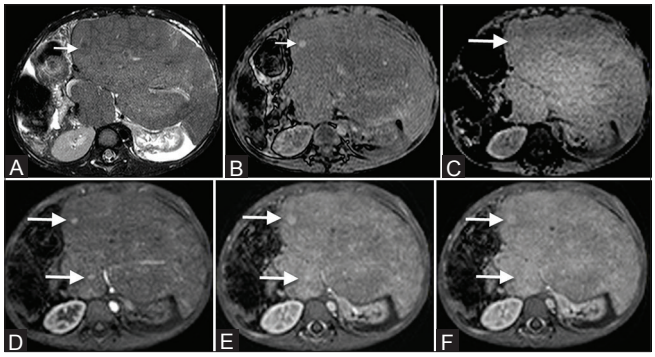

Figure 4 (A-F): Regenerative nodules in a cirrhotic residual liver with previous right lobe resection for hepatoblastoma. Axial T2W fat saturated (A) axial T1W out-phase (B) images, pre-contrast T1W THRIVE image (C) and post-contrast T1W fat saturated images in arterial (D) portal venous (E) and delayed (F) phases show regenerative nodules (arrows). The nodule shows hypointense signal on T2W, hyperintense signal on pre-contrast T1W images, hyper-enhancement on arterial and portal venous phase images, and becomes almost isointense to parenchyma on equilibrium phase images. More nodules are seen on arterial and portal venous phase images; additional nodule is seen on post-contrast images as compared to pre-contrast images in this case. Explanted liver in this child confirmed presence of multiple regenerative nodules

Adenomas

Three children had adenomas, two of which had pathological confirmation. One child proved to have adenomatosis and had normal appearance of background liver parenchyma on MRI; the second one had glycogen storage disorder (GSD) with fatty infiltration of parenchyma; and the third child had polyarteritis nodosa with Budd-Chiari syndrome and cirrhotic liver. The child with adenomatosis had > 10 lesions and remaining two had six lesions each. Fat content was seen in all lesions except one of the lesions in the child with GSD [Figure 5]. Central scar was seen in one lesion. Hemorrhage was seen in the largest lesion in the child with adenomatosis that was resected. Signal characteristics on T1W, T2W, and equilibrium phase images were variable with most lesions showing slight hyper-enhancement on arterial phase images.

Abscesses

Three children, one each with hyper IgE syndrome, GSD, and primary sclerosing cholangitis, had abscesses. Background liver had normal appearance in two and was

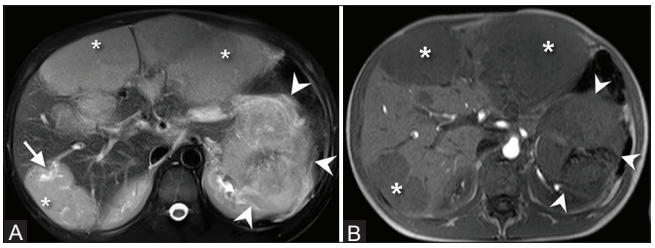

Figure 3(A and B): Multiple hepatic metastases from left renal cell carcinoma. Axial T2W fat saturated (A) and T1W (B) images show multiple lobular masses in the liver (asterisk). One of the lesions shows a scar (arrow on A) within it. The primary tumor in the left kidney (arrowheads) is also seen

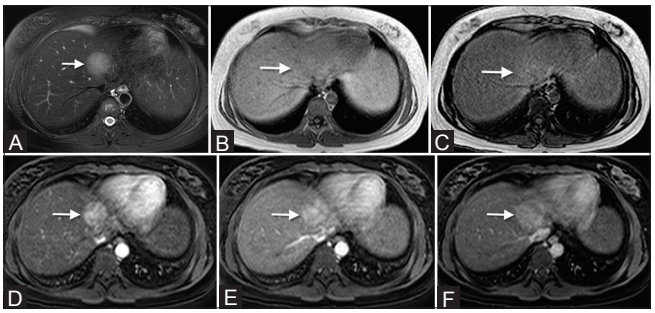

Figure 5 (A-F): Adenomas in a child with glycogen storage disorder. Axial T2W fat saturated (A) axial T1W in-phase (B) axial T1W out-phase (C) images, and post-contrast T1W fat saturated images in arterial (D) portal venous (E) and delayed (F) phases show one of the adenomas (arrows). The lesion shows hyperintense signal on T2W, isointense signal on in- and out-phase images without any fat content, hyper-enhancement on arterial and portal venous phase images, and remains hyperintense to parenchyma on equilibrium phase images. This lesion was biopsied in view of interval increase in size. Pathology showed atypical adenoma. Other five adenomas in this child showed fat content

cirrhotic in one. The largest lesion measured 3.5 × 3.4 cm. Most lesions were hyperintense on T2W images and variable in signal on T1W images. Intravenous contrast was injected in one child during MRI scan that showed ring enhancement of the lesions [Figure 6]. Another child had contrast-enhanced CT scan a day earlier that showed peripheral enhancement. Unfortunately, diffusion-weighted imaging was not performed in the three cases.

Other lesions

Other multifocal liver lesions included one case each of angiomyolipoma in a child with tuberous sclerosis, epithelioid hemangioendothelioma, focal fatty infiltration, hepatocellular carcinoma (HCC), infarcts, nodular regenerative hyperplasia (NRH), and hepatic cysts.

Epithelioid hemangioendotheliomas were seen in a 15-year-old girl with multiple lesions in multiple organs including lungs, liver, and bones. The hepatic lesions were small, peripheral, and showed target appearance on T2W images with central hyperintensity [Figure 7]. They showed initial peripheral enhancement with central enhancement on delayed phase images. There was also hepatic capsular retraction with some of the lesions [Figure 7].

Two foci of HCC were seen in the cirrhotic liver in a child with tyrosinemia. The larger focus showed heterogeneous arterial phase enhancement and washout in equilibrium phase.

Multiple NRH lesions were seen in a child with Alagille syndrome. The background liver was normal on imaging. These nodules were hyperintense on T1W images and hypointense on T2W images relative to hepatic parenchyma. They showed enhancement similar to the parenchyma on all phases.

Multiple infarcts were seen within a cirrhotic liver with portal hypertension in a child with cystic fibrosis [Figure 8]. This case had pathologic confirmation from explanted liver. Right, left, and main portal veins as well as hepatic artery were patent on MRI. These lobulated conglomerate areas were periportal in distribution and showed only minimal smooth peripheral enhancement. They were confused with abscesses on initial imaging review, but clinical features were not fitting with abscesses.

Discussion

Multifocal liver lesions in children include hemangioma, FNH, metastases, hepatoblastoma, mesenchymal hamartoma, adenoma, HCC, infective process, and rarely NRH, epithelioid hemangioendothelioma, and lymphoma.[1-4] The frequency of these lesions in our study does not necessarily represent the true picture because

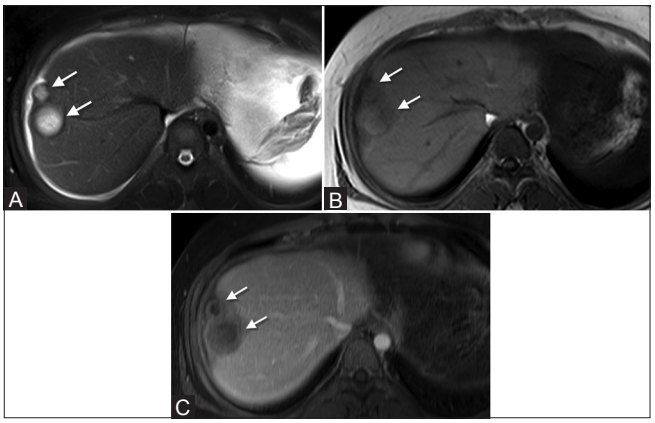

Figure 6 (A-C): Hepatic abscesses in a child with hyper IgE syndrome. Axial T2W fat saturated (A) axial T1W (B) and post-contrast T1W fat saturated (C) images show two conglomerate abscesses in the right lobe (arrows). The lesions show well-circumscribed enhancing wall that is dark on T2W image

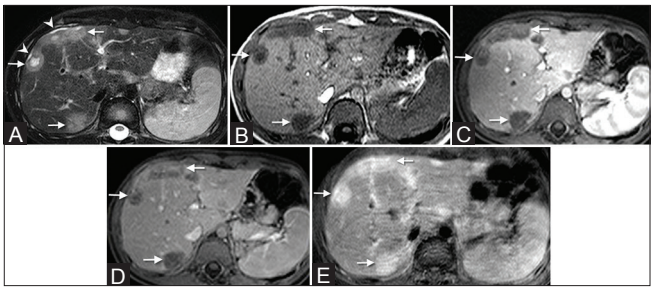

Figure 7 (A-E): Epithelioid hemangioendotheliomas. Axial T2W fat saturated (A) axial T1W in-phase (B) images, and post-contrast T1W fat saturated images in arterial (C) portal venous (D) and delayed (E) phases show multiple lesions (arrows). Some lesions have target appearance with bright center and relatively less bright periphery on T2W image. These peripheral lesions also show capsular retraction (arrowheads). The lesions do not show significant enhancement on arterial phase (C) show only minimal enhancement on portal venous phase (D) and fill completely with homogeneous enhancement on delayed phase image (E) The findings are characteristic for epithelioid hemangioendothelioma (EHE) in this pathologically proved case

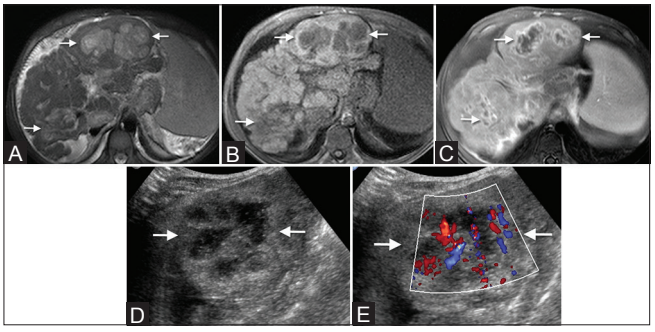

Figure 8 (A-E): Hepatic infarcts. Axial T2W fat saturated (A) axial T1W (B) and post-contrast T1W fat saturated (C) images show multiple lobulated lesions that are predominantly central in location adjacent to portal tracts (arrows). These areas show high signal on T2W (A) low signal on T1W (B) and show smooth peripheral enhancement (C). Gray scale (D) and color (E) ultrasound images show these areas as hypoechoic areas with increased vascularity surrounding them. These infarcts are pathologically confirmed on explanted liver

it evaluates only lesions assessed by MRI and not all the lesions seen in the clinic or a hospital. Not all multifocal lesions are evaluated by MRI at our institution, for example, initial evaluation of suspected hepatoblastoma or stage 4S neuroblastoma is still performed by CT scan that allows staging CT chest and neck to be done in the same short anesthesia time. This is possibly one of the reasons we did not see any cases of multifocal hepatoblastoma and found only one case of multifocal HCC. Nonetheless, barring these exceptions, most liver lesions in children, solitary or multifocal, especially benign lesions, are now increasingly evaluated by MRI at many institutions. Hence, our study represents day-to-day experience in terms of types of lesions seen and their approximate frequency.

FNH was the most common multifocal liver lesion that was evaluated by MRI in our study. FNH is being seen with increasing frequency in children, especially in those who have been previously treated for malignancy.[5-8] FNH tends to be multiple, smaller in size (typically around 2 cm), and most of them lack central scar in these cases.[5-8] It is important to differentiate FNH from metastatic nodules in the liver. Characteristic MRI findings can help avoid biopsy in such situations.[9] Similar to previous reports in the literature, most children with multifocal FNH in our study had history of previous cancer. Most FNH were iso- to hypointense on T1W, slightly hyperintense on T2W, showed prompt arterial enhancement, and became isointense to slightly hyperintense on portal venous phase and equilibrium phase images. Fat-containing FNH were seen in one of our children.

Hemangiomas are the most common benign tumor of infancy and about half of them are multifocal.[3] As reported in the literature, all hemangiomas in our study were hypo- or iso-intense on T1W and hyperintense on T2W images. Peripheral enhancement followed by progressive centripetal enhancement is a typical feature of the hemangioma that can be seen in infantile hepatic hemangioma.[10] However, smaller lesions may not show this feature and may show complete homogenous enhancement of the lesion in the arterial phase itself that is retained on the equilibrium and delayed phase images. This feature was seen in most of our hemangiomas that were small in size with the largest measuring 1.3 × 2.2 cm. These hemangiomas are called "flash hemangiomas." These may be difficult to differentiate from vascular metastases in children with known primary malignancy.

Multiple liver lesions in children, even in those with previous history of cancer, are more likely to represent FNH than metastases as shown in the literature[11] and is reflected in our study. Most common primary tumor for liver metastases in our series was neuroblastoma. Imaging features of metastases are variable and nonspecific on all sequences as shown in this study. Hepatocyte-specific contrast media can help to differentiate them from common benign liver lesion such as FNH.[12,13]

RNs seen in cirrhosis are formed by localized proliferation of hepatocytes and their supporting stroma, and are surrounded by fibrosis.[14] Four of six children with RN in our study had frank changes of cirrhosis on MRI. RN can be micronodular (<3 mm) or macronodular (>3 mm), and are usually <2 cm in size.[15] RNs are typically hypointense on T2W, variable in signal on T1W images, and show enhancement similar to liver parenchyma on all phases including arterial phase.[16] In our study, most nodules were either iso- or hyperintense on T1W images and showed enhancement similar to liver parenchyma. However, on T2W images, four children had hyperintense and two children had hypointense nodules. NRH is a distinct entity from RN of cirrhosis that also shows RNs of hepatocytes seen in non-cirrhotic liver and can be associated with portal hypertension in many cases.[17,18] RNs in NRH are not surrounded by fibrosis. NRH is seen variety of conditions including Budd-Chiari syndrome, congenital anomalies of portal vein, congenital hepatic fibrosis, myeloproliferative and autoimmune disorders, lupus, and chemotherapy among others. The one case of NRH seen in our series had Alagille syndrome.

Hepatocellular adenoma in children is seen with predispositions like use of oral contraceptives in girls, GSD, and anomalies of hepatic vasculature.[1] About 20% of cases with adenoma show multiple lesions.[3] Adenomas have been classified into three types: 1. Inflammatory, 2. hepatocyte nuclear factor 1 alpha-mutated, and 3. beta-catenin–mutated adenoma.[19] The inflammatory subtype is predisposed for hemorrhage, while inflammatory and beta-catenin-mutated subtypes are at risk for developing into HCC in up to 5-10% cases.[19] Fat content, suggested by signal drop on out-of-phase image, is the characteristic feature of adenomas. However, inflammatory subtype may not show this feature. Most adenomas are hyperintense on T1W and T2W images and show hyper-enhancement in the arterial phase. They become isointense to hepatic parenchyma on delayed phases. However, appearances can be variable.

Even though not seen in our series, hepatoblastoma can be multifocal in 20% of cases.[4] Similarly, HCC also can be multifocal. One such case of HCC was seen in our series. Hepatic abscesses are typically seen in immunocompromised children, especially those with immunodeficiencies, those on various cancer therapies, or recipients of transplantation. Peripheral enhancement and perilesional edema along with clinical features help to differentiate abscesses from other lesions. They are restricted on diffusion. Metastases have variable imaging features. One of the common causes of hepatic metastases in children is neuroblastoma in which the liver is markedly enlarged. Other rare cases of multifocal liver lesions were seen in our series including epithelioid

hemangioendothelioma that showed characteristic imaging features described in the literature.[20]

Limitations of this study include retrospective nature and lack of pathologic confirmation in many cases. Most cases without pathologic confirmation were of FNH and hemangioma. However, because of common occurrence and typical MRI features in most cases, FNH are mainly diagnosed by MRI and are rarely biopsied.[7] One of the limitations of this study was lack of cases with imaging using hepatocyte-specific contrast media that have improved sensitivity and specificity of non-invasive diagnosis of hepatic lesions in children and adults.

Conclusion

Multifocal liver lesions are uncommonly seen in children and include common and uncommon pathology. MRI can be used for evaluation of multiple liver lesions in children. It helps achieve reasonable differential diagnoses and guide further investigation and management. In some cases, MRI features may obviate invasive liver biopsy.

References

1. Hegde SV, Dillman JR, Lopez MJ, Strouse PJ. Imaging of multifocal liver lesions in children and adolescents. Cancer Imaging 2012;12:516-29.
2. Duigenan S, Anupindi SA, Nimkin K. Imaging of multifocal hepatic lesions in pediatric patients. Pediatr Radiol 2012;42:1155-68; quiz 1285.
3. Chung EM, Cube R, Lewis RB, Conran RM. From the archives of the AFIP: Pediatric liver masses: Radiologic-pathologic correlation part 1. Benign tumors. Radiographics 2010;30:801-26.
4. Chung EM, Lattin GE Jr, Cube R, Lewis RB, Marichal-Hernández C, Shawhan R, *et al*. From the archives of the AFIP: Pediatric liver masses: Radiologic-pathologic correlation. Part 2. Malignant tumors. Radiographics 2011;31:483-507.
5. Do RK, Shaylor SD, Shia J, Wang A, Kramer K, Abramson SJ, *et al*. Variable MR imaging appearances of focal nodular hyperplasia in pediatric cancer patients. Pediatr Radiol 2011;41:335-40.
6. Bouyn CI, Leclere J, Raimondo G, Le Pointe HD, Couanet D, Valteau-Couanet D, *et al*. Hepatic focal nodular hyperplasia in children previously treated for a solid tumor. Incidence, risk factors, and outcome. Cancer 2003;97:3107-13.
7. Benz-Bohm G, Hero B, Grossmann A, Simon T, Körber F, Berthold F. Focal nodular hyperplasia of the liver in longterm survivors of neuroblastoma: How much diagnostic imaging is necessary? Eur J Radiol 2010;74:e1-5.
8. Towbin AJ, Luo GG, Yin H, Mo JQ. Focal nodular hyperplasia in children, adolescents, and young adults. Pediatr Radiol 2011;41:341-9.
9. Valentino PL, Ling SC, Ng VL, John P, Bonasoni P, Castro DA, *et al*. The role of diagnostic imaging and liver biopsy in the diagnosis of focal nodular hyperplasia in children. Liver Int 2014;34:227-34.
10. Kassarjian A, Zurakowski D, Dubois J, Paltiel HJ, Fishman SJ, Burrows PE. Infantile hepatic hemangiomas: Clinical and imaging findings and their correlation with therapy. AJR Am J Roentgenol 2004;182:785-95.
11. Smith EA, Salisbury S, Martin R, Towbin AJ. Incidence and etiology of new liver lesions in pediatric patients previously treated for malignancy. AJR Am J Roentgenol 2012;199:186-91.
12. Seale MK, Catalano OA, Saini S, Hahn PF, Sahani DV. Hepatobiliary-specific MR contrast agents: Role in imaging the liver and biliary tree. Radiographics 2009;29:1725-48.
13. Chavhan GB, Mann E, Kamath BM, Babyn PS. Gadobenate-dimeglumine-enhanced magnetic resonance imaging for hepatic lesions in children. Pediatr Radiol 2014;44:1266-74.
14. Hussain SM, Reinhold C, Mitchell DG. Cirrhosis and lesion characterization at MR imaging. Radiographics 2009;29:1637-52.
15. Hanna RF, Aguirre DA, Kased N, Emery SC, Peterson MR, Sirlin CB. Cirrhosis-associated hepatocellular nodules: Correlation of histopatholgic and MR imaging features. Radiographics 2008;28:747-69.
16. Hussain SM, Zondervan PE, IJzermans JN, Schalm SW, de Man RA, Krestin GP. Benign versus malignant hepatic nodules: MR imaging findings with pathologic correlation. Radiographics 2002;22:1023-39.
17. Gentilucci UV, Gallo P, Perrone G, Del Vescovo R, Galati G, Spataro S, *et al*. Non-cirrhotic portal hypertension with large regenerative nodules: A diagnostic challenge. World J Gastroenterol 2011;17:2580-4.
18. Dachman AH, Ros PR, Goodman ZD, Olmsted WW, Ishak KG. Nodular regenerative hyperplasia of the liver: Clinical and radiologic observations. AJR Am J Roentgenol 1987;148:717-22.
19. Katabathina V, Menias CO, Shanbhougue AK, Jagirdar J, Paspulati RM, Prasad SR. Genetics and imaging of hepatocellular adenomas: 2011 update. Radiographics 2011;31:1529-43.
20. Dong A, Dong H, Wang Y, Gong J, Lu J, Zuo C. MRI and FDG PET/CT findings of hepatic epitheloid hemangioendothelioma. Clin Nucl Med 2013;38:e66-73.

Cite this article as: Almotairi M, Oudjhane K, Chavhan GB. Pediatric multifocal liver lesions evaluated by MRI. Indian J Radiol Imaging 2015;25:296-302.

Source of Support: Nil, **Conflict of Interest:** No.